Journal of
Engineering Sciences
Faculty of Engineering
Assiut University
JES
مجلة
العلوم الهندسية
كلية الهندسة
جامعة أسيوط
journal homepage: http://jesaun.journals.ekb.eg

Flexural Behavior of Concrete Box Girders Reinforced with Mixed Steel and Basalt Fiber-Reinforced Polymer

Received 21 October 2021; Revised 1 April 2023; Accepted 1 April 2023

Hemdan O. A. Said[1]
Mahmoud A. M. Hassanean[2]
Yahia A. Hassanean[3]
Arafa M. A. Ibrahim[4]

Abstract

This paper presents the flexural behavior of reinforced concrete box (RCB) girders reinforced with both steel and fiber-reinforced polymer (FRP). An experimental study was conducted on five RCB girders. The first two girders were reinforced in the tension side with either steel or basalt FRP (BFRP) bars, while the other three ones were reinforced with both steel and BFRP bars with various BFRP-to-total reinforcement ratios (A_f/A_t). The RCB girders were tested under four-point monotonic static loading and the main fundamental characteristics of the proposed reinforcement were investigated. The experimental results showed that increasing the A_f/A_t ratio improved both the ultimate load and the deflection at failure, while the ductility index decreased. Comparing the obtained RCB test results with those found in the literature of the ordinary beams revealed that the behavior is almost identical. With the range of the experimental investigations conducted in this study, a value of about 50% to 70% for A_f/A_t ratio is recommended in the design of hybrid RCB girders as it provides enough post elastic strength and stiffness for meeting the ductility requirement. Ultimately, the application of the analytical structural approach available in the literature was adopted to predict the flexural capacity of mixed RCB girders and good agreement with the experimental results was proved.

Keywords
Reinforced concrete box girders; Reinforcement ratio; Mixed steel and BFRP bars; Ductility index; Ordinary beams; Analytical design

1. Introduction

Box girder Bridges nowadays has achieved a prominently usage in the construction industry. It gained this popularity due to its accelerated construction, high flexural and torsional stiffness, serviceability, favorable depth-to-weight ratio, aesthetic shape, and economical-effectiveness [1-6]. As a member of reinforced concrete (RC) bridges, RC box (RCB) girders are directly exposed to the air and sometimes to the detrimental gasses from the ecological contaminants. Accordingly, the steel reinforcements of these members are being liable to corrosion. Corrosion of steel bars

[1] okasha73@eng.svu.edu.eg - Assistant Professor, Civil Eng., Dept., Faculty of Eng., South Valley University, Egypt
[2] mahmoud_abdo@eng.svu.edu.eg - Assistant Professor, Civil Eng., Dept., Faculty of Eng., South Valley University, Egypt
[3] yehia.mekhaimer@eng.au.edu.eg - Professor, Civil Eng., Dept., Faculty of Eng., Assiut University, Egypt
[4] arafa_mahmoud@eng.svu.edu.eg - Assistant Professor, Civil Eng., Dept., Faculty of Eng., South Valley University, Egypt

https://doi.org/10.21608/JESAUN.2023.170121.1176

entrenched in RC structures declines their durability and serviceability as well as longevity and instigates prompt structural failure, which is considerably costly to inspect as well as to restore [7]. Moreover, the well-known elasto-plastic material property of steel reinforcement has been emphasized as another drawback of steel reinforcements, especially for constructions located in high seismic zones. The elasto-plastic property of steel reinforcements limits their ability to continue carrying load after yielding and restricts their efficiency in structures that to be designed with high strength and post-earthquake recoverability [8-10]. Therefore, significant research efforts have been done in the last decades aiming to replace the steel reinforcements by effective construction materials.

Recently, there has been a growing trend in using fiber reinforced polymer (FRP) composites as an effective alternative for steel reinforcements in RC structures. FRP has gained their application demand due to their advantages comparing with steel reinforcements including corrosion resistance, high strength, light weight, perfect non-magnetizing characteristics, and ease of application. Several investigations have emphasized the efficiency of FRP composites as strengthening and rehabilitation of existing steel-RC members as well as reinforcing materials for new structures [11-19]. The results of those research have shown that the linear elastic material property and the low modules of elasticity of FRP reinforcements greatly limits the ductility and serviceability of FRP RC structures. The results have also proven that FRP RC structures suffer from wide cracks and large formations compared to steel RC ones. Furthermore, two main failure modes of FRP RC structures were reported depending on the amount of the FRP reinforcement, where failure due to rupture of FRP bars or due to concrete crushing, have been classified for under-reinforced or over-reinforced sections, respectively. Following the existing research studies, design guides and recommendations have been developed for FRP RC structures and over-reinforced sections were called for such structures to enhance their deformability and ductility [20-21].

Recently, hybrid RC systems by combining both the steel and FRP bars have been proposed to overcome the durability, serviceability, and ductility of purely steel or FRP RC structures [22-34]. Research studies carried out in hybrid steel-FRP RC bridge columns showed that the proposed hybrid system could realize a stable post-yield stiffness and a reasonable ductility before failure. The ductility and serviceability of that systems were ensured by the steel reinforcement, while the ultimate strength was reached by the FRP reinforcement. Similar remarks were also reported in hybrid steel FRP beams [8,25]. In this direction, some research studies have focused on finding out the nominal steel and FRP reinforcement ratios in hybrid RC beams, e.g., a range of 1 to 2.5 for A_f/A_s (FRP to steel reinforcement ratio) was recommended for better stiffness and ductility [31], while a range of 1 to 2 was recommend for sufficient energy absorption [33]. Other research studies [23,33] developed a deformability index, as an alternative indicator for the ductility, of hybrid-RC beams and it was found that it reduces with increasing the A_f/A_s ratio. Similarly, another numerical study [26] emphasized the responsibility of steel-to-FRP reinforcement ratio for controlling the strength, stiffness, and deformability of hybrid beam-column joints and reported its role in the design of such joints.

To this end, hybrid reinforcement of steel and FRP bars have been adopted as an effective RC system for modern structures and great research efforts have been done on hybrid RC beams, columns, and beam-column joints. Even though, enough research results on hybrid steel FRP RCB girders have not been published yet. Therefore, a research project is ongoing aiming to fill in this gap and the objective of the current study as a part of this project was to explore experimentally the fundamental characteristics of the flexural behavior of hybrid steel-FRP RCB girders.

2. Experimental Program

An experimental program was carried out on a total of five RCB girders reinforced in tension with different combinations of steel and BFRP bars. Along with the tested specimens, one steel RC specimen (BS) was designed according to AASHTO LFRD (2010) [35] and served as a reference specimen, while another four steel-BFRP RC specimens were designed to give higher strengths when compared to the reference girder.

2.1. Materials

A target concrete compressive strength (f_{cu}) of 35 MPa was implemented for all examined samples. Table 1 demonstrates the quantity of the implemented concrete mix. Table 2 exhibits the mechanical characteristics of steel and BFRP bars, those were experimentally obtained according to the ACI specifications [15], employed in the investigational program. The yield strength (f_y) as well as the ultimate strength (f_u) of the 12-mm-diameter deformed steel bars employed as longitudinal tension reinforcement were 490 and 590 MPa, respectively. The corresponding values for the 10-mm-diameter steel compressive reinforcement were 480 and 610 MPa, respectively. Likewise, the corresponding values for the 8-mm-diameter smooth steel transverse reinforcement were 270 and 378 MPa, respectively as given in Table 2. Additionally, the ultimate rupture strength and modulus of elasticity of 12-mm-diameter BFRP bars were 1060 Mpa and 48 Gpa, respectively.

Table 1: The proportion of the concrete mix.

f_{cu} MPa	Cement kg/m^3	Sand kg/m^3	Gravel size kg/m^3	Water Liter/m^3
35	450	608.7	1126	202

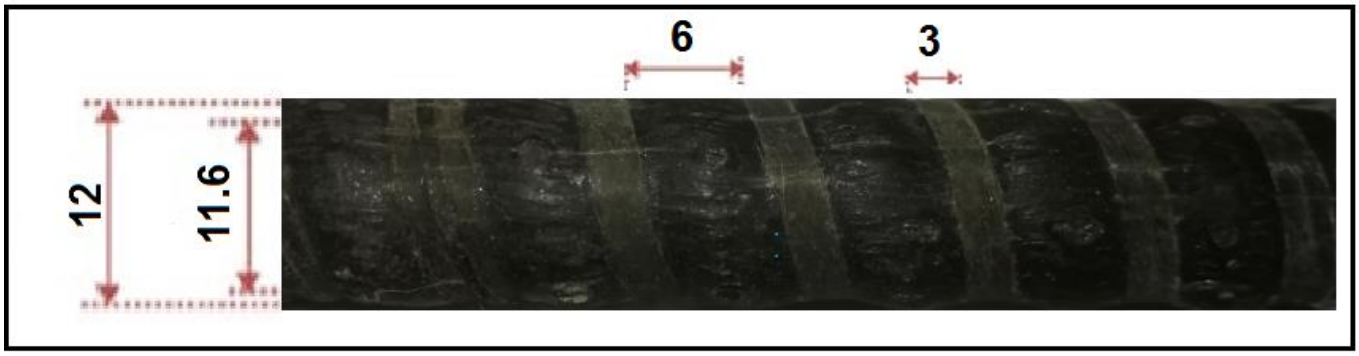

Fig. 1. Configuration of the surface texture of the Basalt FRP bar.

Table 2: Mechanical Properties of steel and Basalt FRP bars.

Steel Type	Diameter (mm)		Yield or proof Strength. (f_y) MPa	Ultimate Strength (f_u) Mpa	Modulus of elasticity (E_s) Gpa
	Nominal diameter	Actual diameter			
MS	8.00	8.00	270	378	200
HTS	10.00	10.07	480	610	200
HTS	12.00	12.05	490	590	200
BFRP	12.00	12.00	-	1061	48.2

MS means Mild Steel and HTS means High Tensile Steel

2.2. Test specimens and experimental parameters

The examined RCB girders had an overall length of 3000 mm as well as a clear span of 2700 mm. The cross section was a rectangular hollow one of external and internal dimensions of 400 mm width ×400 mm height as well as 200 mm width × 200 mm height, respectively, as shown in Figs. 2 and 3. These girder sizes were designated based on the obtainable facility capability of the RC organization research laboratory in the National Housing and Building Research Center (NHBRC) in Cairo, the test center where the examinations were carried out. All girders in this study were reinforced at the top with 4 steel bars of 10-mm diameter, while the shear reinforcement consisted of 8-mm-diameter internal closed stirrups at 200 mm intervals. The configuration of the surface texture of the BFRP bar is shown in Fig. 1. According to the tension reinforcement type and combinations, five diverse RCB girders were investigated to meet the aim of this research. As shown in Figs. 2 to 5 and Table 3, a detailed description of the test specimens are as follows:

- Sample BS (Fig. 3a) functioned as a reference sampling. In this girder, the flexural steel reinforcement comprised of six 12-mm-diameter bars with A_f/A_t ratio equivalent to 0.00, where A_t is the total cross-sectional areas of steel and BFRP bars, whereas A_f is the total cross-sectional areas of BFRP bars.
- Sample BSF-0.33F (Fig. 3b) was strengthened with the identical area of reinforcement as sample BS. Though, two steel bars were substituted with two BFRP bars of identical diameter creating an A_f/A_t ratio of 0.33.
- Sample BSF-0.50F (Fig. 3c) was strengthened with the identical area of reinforcement as sample BS. Nevertheless, three steel bars were substituted with three BFRP bars of the same diameter creating an A_f/A_t ratio of 0.50.
- Sample BSF-0.67F (Fig. 3d) was strengthened with the similar area of reinforcement as sample BS. Nonetheless, four steel bars were substituted with four BFRP bars of identical diameter creating an A_f/A_t ratio of 0.67.
- Sample BF (Fig. 3e) was strengthened with the similar area of reinforcement as sample BS. Yet, six steel bars were substituted with six BFRP bars of identical diameter creating an A_f/A_t ratio of 1.00.

Table 3: Details of the tested box girders

Girder ID	$f_{cu,actual}$ MPa	A_f No. of bars	A_s No. of bars	A_t No. of bars	A_f/A_t ratio	Type of tension reinforcement
BS	36.0	0	6Φ12	6Φ12	0.00	Steel
BSF-0.33F	35.0	2Φ12	4Φ12	6Φ12	0.33	Steel + BFRP
BSF-0.50F	35.5	3Φ12	3Φ12	6Φ12	0.50	
BSF-0.67F	36.0	4Φ12	2Φ12	6Φ12	0.67	
BF	36.0	6Φ12	0	6Φ12	1.00	BFRP

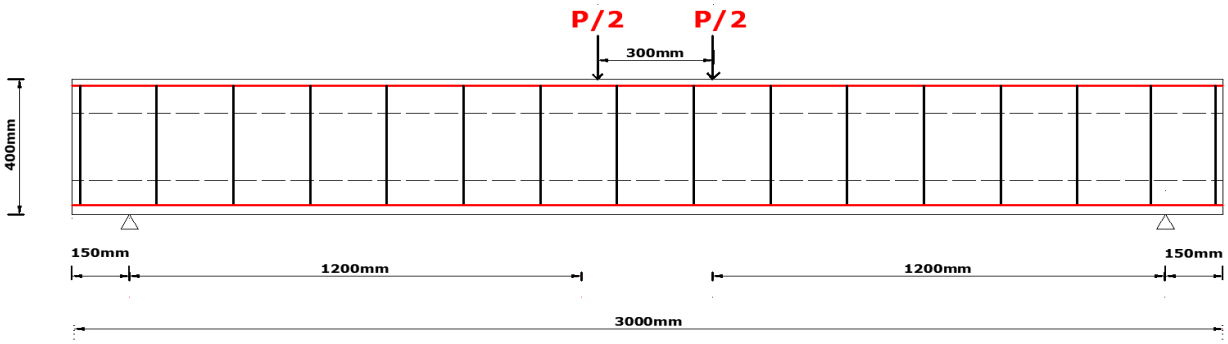

Fig. 2. Geometrical dimensions, reinforcement details, and loading conditions of a typical test specimen.

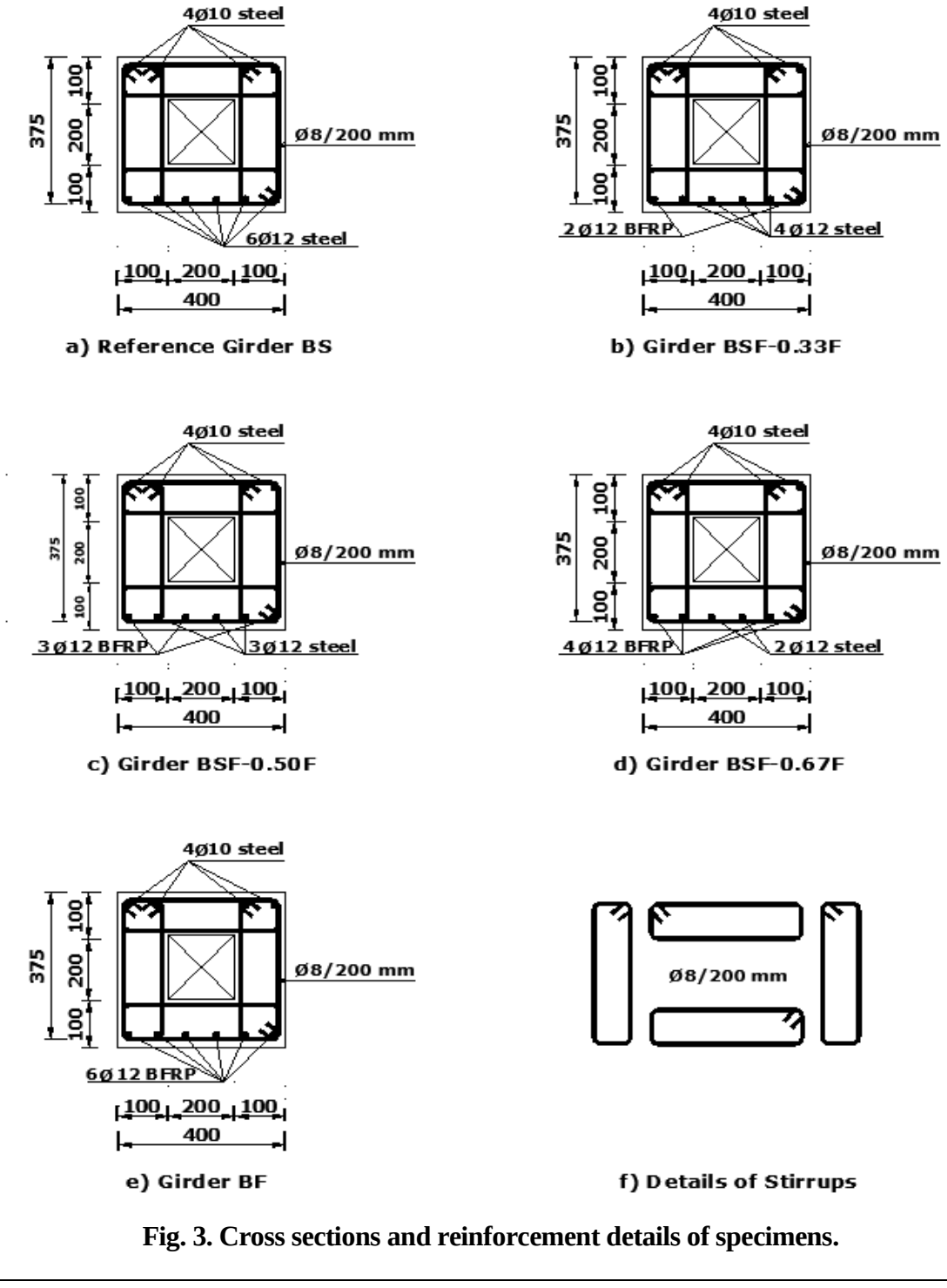

Fig. 3. Cross sections and reinforcement details of specimens.

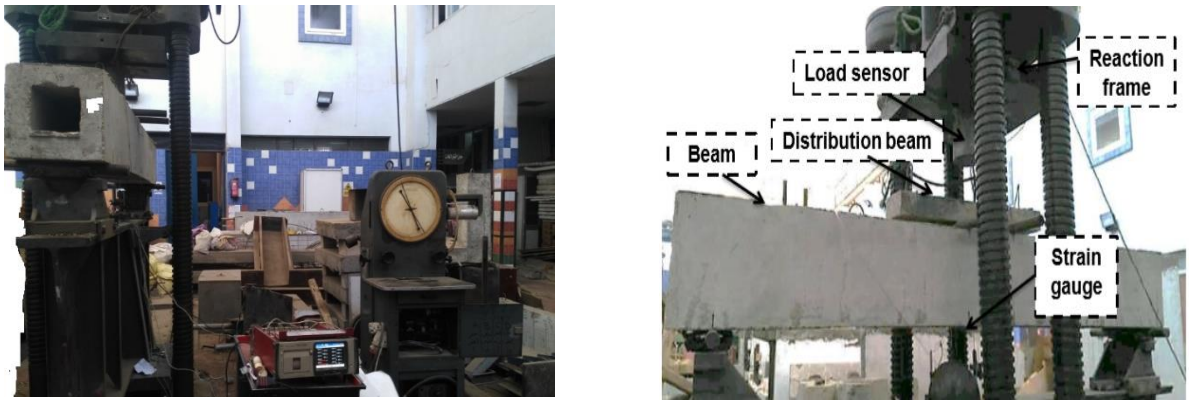

Fig. 4. Set up of the tested box girders.

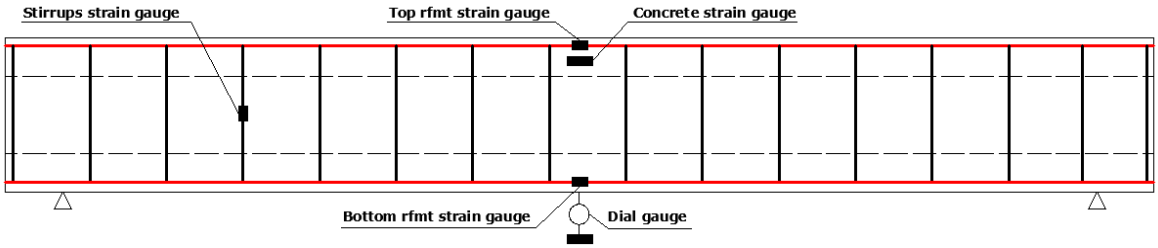

Fig. 5. Instrumentation of the tested girders.

2.3. Loading and instrumentations

The setup of the tested box girders is shown in Fig. 4. All girders were tested under four-point bending over a clear span of 2700 mm as shown in Fig. 2. The deflection at midspan was measured utilizing a dial gauge with accuracy of 0.01 mm. The dial gauge was fixed on the bottom surface at the midspan of the tested girders to achieve an accurate measurement as shown in Fig. 5.

The induced strains in the longitudinal bottom BFRP and/or steel bars, top steel bars, and strains in stirrups were measured using electrical strain gauges. The strain gauges had a 350 ohms resistance, 2.04 gauges factor, and a length of 15 mm. The strain gauges were attached to the bottom surface of reinforcement at midspan for longitudinal reinforcement and at 600 mm from the edge of the girders for stirrups. Moreover, electrical strain gauges with 6o mm length were used to measure the strains in the compressive zone of concrete, as shown in Fig. 5.

3. Test Results

3.1. Crack patterns and failure modes

The commencements as well as propagation of cracks for the diverse examined box girders were witnessed visually with an amplifying glass. For all girders, it was noted that the cracks on both sides of those girders were almost alike. The cracks were principally originated at the lower side in the constant moment zone. The primary detected crack stretched up to a point greater than half of the girder depth. As the load amplified, these cracks broadened and spread upward. Far along, novel cracks began along the lower side of the girder and disseminated in the direction of the position of the load administration. For the reference girder BS that had only steel bars, the first crack commenced at a load of 60.0 kN. Afterwards, the quantity of cracks amplified and spread upward till the steel bars came to yielding at a load of 190.0 kN. The cracks augmented and started to be broader up until the concrete crushed at the top side that caused the failure of the girder at a load of 233.5 kN. The girder BS destructed primarily by yielding of steel prior to concrete crushing as demonstrated in Table 4 and (Fig. 6.a).

For the BFRP RC girder (BF), the first crack commenced at a load of 50.0 KN. Afterwards, the quantity of cracks amplified and disseminated upward till the BFRP bars came to their rupture strain; the cracks amplified and became broader till the concrete crushed at the top side, which caused the failure of the beam at a load of 348.9 kN. The cracks' height as well as width in the girder BF was grander than those of the girder BS as demonstrated in (Figs.6.a, and 6.e). The girder BF failed primarily by the rupture of BFRP reinforcing bars followed by concrete crushing.

Similar behavior of the girder BF was detected for the hybrid girders BSF-0.33F, BSF-0.50F, as well as BSF-0.67F (reinforced with mixed steel and BFRP bars) with A_f/A_t ratios equivalent to 0.33, 0.50, and 0.67, respectively. The primary crack commenced at loads of 58.0 kN, 56.0 kN, and 53.0 kN, respectively. Correspondingly, the steel bars yielded at loads of 160.0 KN, 146.0 kN, and 138.0 kN, respectively; and the girders reached their ultimate state at loads of 281.1 kN, 296.2 kN, and 336.3 kN, respectively. Similarly, the failure manner was in a flexural mode as demonstrated in (Figs. 6.b, 6.c, and 6.d). The number of cracks at failure in the hybrid RCB girders was greater than that of the reference girder which was reinforced with steel bars only (girder BS). Moreover, the height as well as width of the cracks in the girder reinforced only with BFRP bars were grander than those of the whole other girders. The cracks transmitted rapidly in the girders which were reinforced either entirely or partly with BFRP bars. The height of the primary crack was considerably influenced by the area of steel bars. For instance, the height of the primary cracks for the hybrid RCB girders BSF-0.33F, that had an A_f/A_t ratio equivalent to 0.33, BSF-0.50F, that had an A_f/A_t ratio equivalent to 0.50, as well as BSF-0.67F, that had an A_f/A_t ratio equivalent to 0.67, were 71%, 83%, and 90% of that of the reference girder BS, respectively.

The hybrid RCB girders (BSF-0.33F, BSF-0.50F, as well as BSF-0.67F) which had similar total area of reinforcement failed because of steel yielding followed by the rupture of BFRP bars. Yet, the failure manners of the hybrid RCB girders were additionally ductile than in the BFRP RCB girder BF. Moreover, it was found that the crack patterns and failure modes of RCB girders reinforced with mixed steel and BFRP bars in the current study agree well with the observations of many previous research studies carried out on solid RC beams [36]. Through the observations of the current study and the previous ones, it was found that the cracking spacing, and width are controlled by the amount of steel and FRP reinforcements. the typical crack spacing of steel-RC beams was marginal, the regular crack spacing of FRP-RC beams was the highest, and the regular crack spacing of hybrid RC beams was someplace in the mid. At similar ultimate bearing capacity as well as identical loading, the regular crack spacing lessens with the decline of A_f/A_t.

Table 4: Test results of the tested box girders

Girder ID	P_{cr} kN	P_y kN	P_u kN	Δ_{cr} (mm)	Δ_y (mm)	Δ_u (mm)	$\acute{\varepsilon}_{su}$	$\acute{\varepsilon}_{fu}$	$\acute{\varepsilon}_{cu}$	Mode of failure
BS	60.0	190.0	233.5	1.10	7.40	80	0.020	-	0.003	SY followed by CC
BSF-0.33F	58.0	160.0	281.1	1.50	7.60	62	0.019	0.022	0.003	SY, CC, and BFRP rupture
BSF-0.50F	56.0	145.6	296.2	1.35	8.00	57	0.010	0.022	0.003	SY, CC and BFRP rupture
BSF-0.67F	53.0	138.0	336.3	1.60	8.20	54	0.008	0.022	0.003	SY, CC, and BFRP rupture
BF	50.0	-	348.9	1.85	-	52	-	0.022	0.003	CC and BFRP rupture

$\acute{\varepsilon}cu$ = the ultimate compressive strain in concrete; $\acute{\varepsilon}fu$ = the ultimate tensile strain in FRP bars; and $\acute{\varepsilon}su$ = the ultimate tensile strain in steel bars; SY= Steel Yielding; CC= Concrete Crushing.

a) Girder BS.

c) Girder BSF-0.33F.

d) Girder BSF-0.50F.

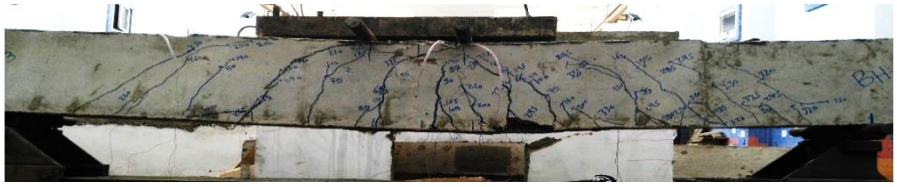

e) Girder BSF-0.67F.

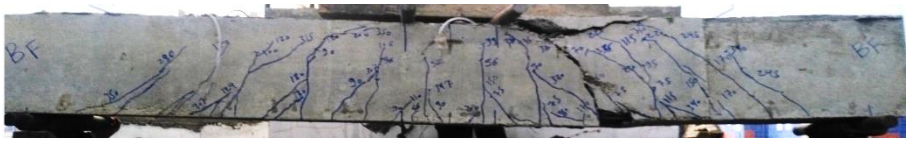

f) Girder BF.

Fig. 6. Modes of failure of the tested girders.

3.2. Load deflection relationship

Fig. 7 illustrates the structural performance of the tested girders through their load-midspan deflection relationships. for the diverse examined box girders. This illustration demonstrates that the performance of all girders started with a linear portion up to the initiation of concrete cracking at the position of maximum tensile stress. Following the initial cracking, the subsequent section of the load-deflection curves deviated to a smaller stiffness. This deviation declines as the ratio of A_f/A_t rises. The surge in deflection after primary cracking is being more pronounced in the girder reinforced with BFRP solely comparing with other girders, e.g., at 90% of the ultimate load, the deflection of the girder reinforced with BFRP bars only is approximately 250% greater than that of the girder reinforced with steel bars solely, as presented in Fig. 7. Furthermore, in this demonstration, the deflection at failure in the hybrid girders BSF-0.33F, BSF-0.50F, as well as BSF-0.67F is somewhat greater than that of the girder BS. For the examined box girders, the recorded deflection at ultimate load amplified as the A_f/A_t ratio lessened.

Again, the flexural structural performance of RCB girders with different combinations of steel and BFRP reinforcements agreed well with the results and observations of the past investigations carried out on similar solid RC beams. E.g., it was observed in the study of Qu et al. 2009 [31] that the initial pre-cracking stiffness of the beams is the same whether the type of reinforcement is steel, FRP, or hybrid. While the post-cracking stiffness significantly depends on the effective reinforcement ratio, i.e., the smallest effective reinforcement ratio the smallest post-cracking stiffness.

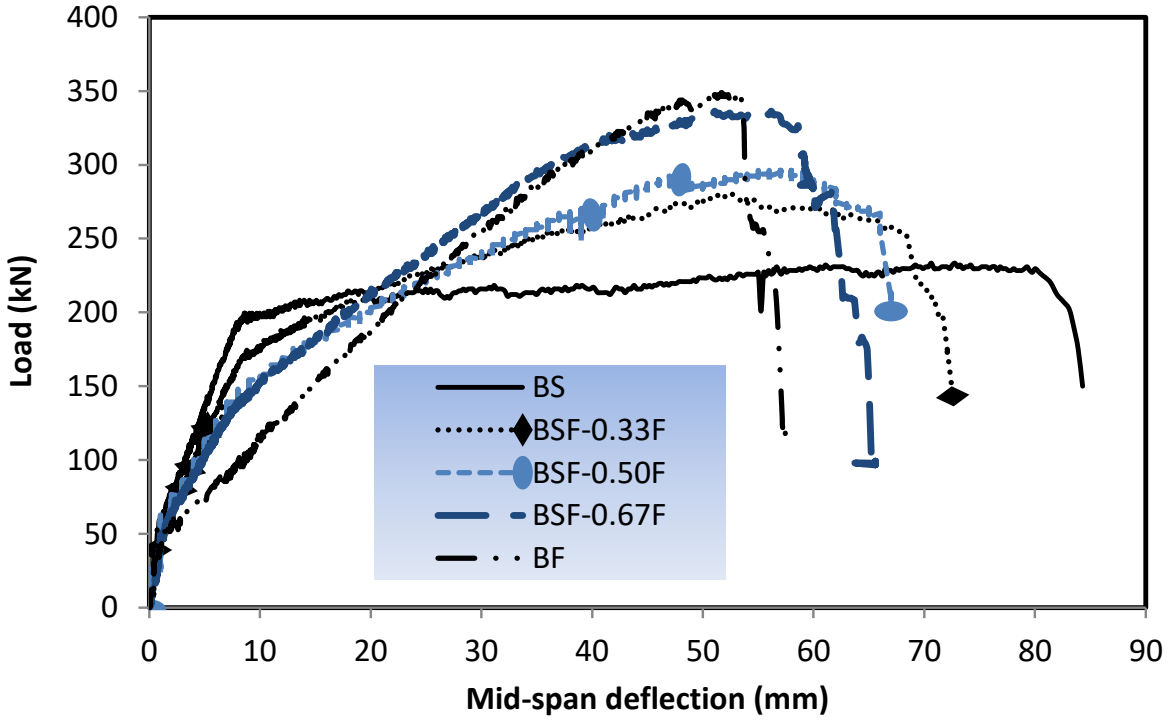

Fig. 7. Effect of A_f/A_t ratio on loads and deflections.

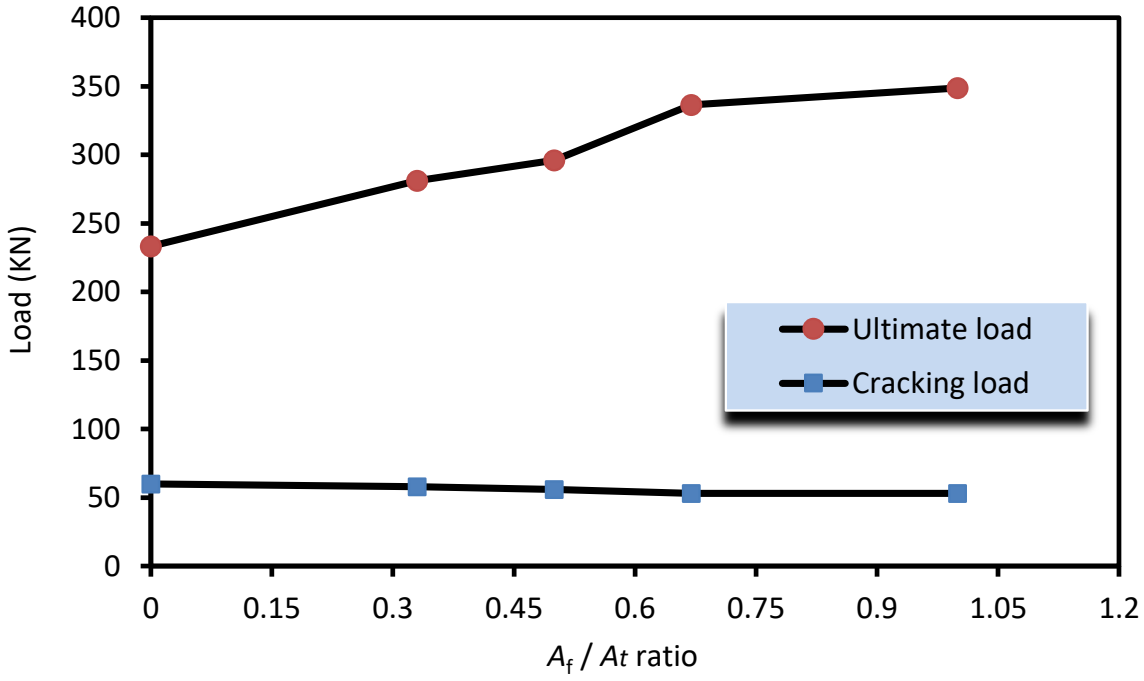

Fig. 8. Effect of A_f/A_t ratio on cracking and ultimate loads.

4. Analysis and Discussion of Test Results

In the light of test results, this section describes the effect of BFRP reinforcement ratio, A_f/A_t, on the strength, ductility, energy absorption, and reinforcement strain of the tested RCB girders.

4.1. Effect of A_f/A_t ratio on the strength of box girders

Table 5 summarized the cracking and ultimate loads of the tested girders and Figs. 8 and 9 shows the effect of A_f/A_t ratio on both the cracking and ultimate strengths of the girders. The cracking load of whichever, the girders reinforced solely with steel bars or hybrid reinforcements, is to some extent higher than the cracking load of the girder reinforced solely with BFRP bars. Furthermore, the A_f/A_t ratio exhibited a substantial impact on the ultimate load of the examined girders having similar total area of reinforcement. The ultimate load of box girders BSF-0.33, BSF-0.50, BSF-0.67, as well as BF having A_f/A_t ratios of 0.33, 0.50, 0.67, and 1.00 are around 1.20, 1.27, 1.44, and 1.49 times the ultimate load of the steel-RCB girder BS, respectively. This proves that as the A_f/A_t ratio surges, the ultimate load likewise rises. This is attributable to the greater tensile stress of BFRP bars comparing with steel bars.

From the load-deflection curves given in Fig. 7, it is obvious that the stiffness of the hybrid RCB girders is small and decreases quickly after cracking. It is evidence from the deflection curves that as the A_f/A_t ratio, with constant reinforcement area, increased, the deflection at failure of the girder decreased. Also, it is noticed that the deflections of the hybrid box girders at any load level are smaller than the deflection of the BFRP box girders. This may be attributed to the low elastic modulus of BFRP bars compared with the elastic modulus of steel bars.

Table 5: Cracking and ultimate loads of the tested box girders

Girder ID	f_{cu} N/mm2	A_f	A_s	A_t	A_f/A_t ratio	P_{cr} (kN)	P_u (kN)	P_u/P_{cr}
BS	36	0	6Φ12	6Φ12	0.00	60.0	233.5	3.89
BSF-0.33F	35	2Φ12	4Φ12	6Φ12	0.33	56.0	296.2	4.85
BSF-0.50F	35.5	3Φ12	3Φ12	6Φ12	0.50	58.0	281.1	5.29
BSF-0.67F	36	4Φ12	2Φ12	6Φ12	0.67	53.0	336.3	6.35
BF	36	6Φ12	0	6Φ12	1.00	50.0	348.9	6.98

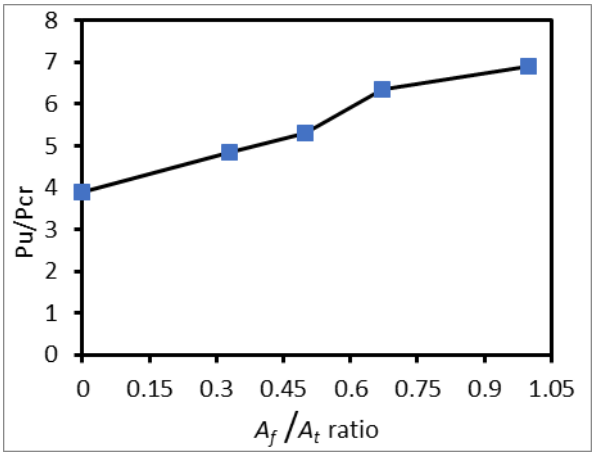

Fig. 9. Effect of A_f/A_t ratio on the ultimate-to-cracking-load ratio at constant reinforcement area.

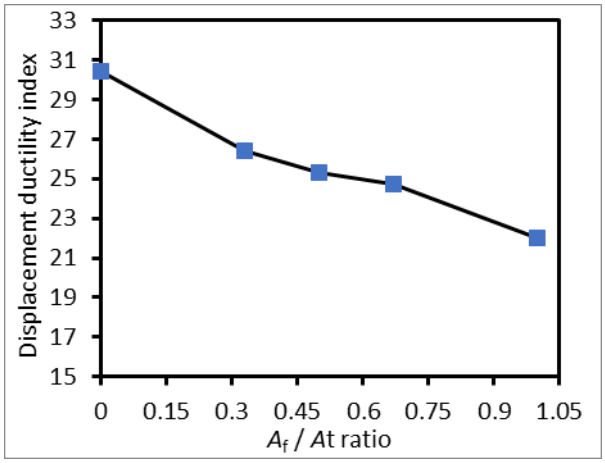

Fig. 10. Effect of A_f/A_t ratio on the ductility.

4.2. Effect of A_f/A_t ratio on the ductility and energy absorption of box girders

Besides the strength demand, ductility and energy absorption are two important structural performance indices in design of modern concrete structures, and they have been emphasized as structural design requirements in most design codes. In this concern, the term "ductility" refers to the ability of structures to undergo inelastic deformation before failure without respectable drop in their strength or may refer to the ability of absorb energy without significant deterioration before failure [37-38]. In general, respect of the obtainable ductility of a structure is essential for the subsequent reasons: (a) to avoid brittle failure, (b) to employ dispersals of bending moments contradictory from that acquired from linear elastic structural analysis, in addition to (c) surviving a severe seismic activity as well as blast loading. The ductility of RC beams can be calculated according to structural features such as mid-span deflection, curvature, or energy absorption capacity as exemplified by the area below the load-deflection curve. In this study, the traditional displacement ductility index [$\mu_D = \Delta_u/\Delta_y$], was employed to quantify the ductility of steel and hybrid RCB girders; where, Δ_u and Δ_y are the midspan deflections at ultimate state and steel yielding state, respectively. This definition of ductility is clearly not appropriate for BFRP-RC girder, as there is no clear yield point for the reinforcing bars of this specimen [23].

Aiming at overcoming the problem of inability of applying the traditional ductility index in FRP RC structures, two main approaches; namely: Energy-based approach and Deformation-based approach, have been widely used as alternative indices to the ductility [39-40]. In the energy-based approach, ductility is expressed as the ratio of total energy computed as the area under the load deflection curve up to failure to the elastic energy which released at failure. The Deformation-based approach, which is also known as the J-factor approach, is defined as the ratios of the products of moment and curvature at ultimate state to that at a concrete compressive strain of 0.001. In this approach, the condition where the compressive strain of concrete reaches 0.001 is considered as the onset of inelastic deformation of the concrete member and is considered as the equivalent point of structural yield.

By reviewing the findings of wide experimental investigations found in the literature, it was emphasized that the ductility indices computed by the approaches are quite different [e.g., 41]. Additionally, through the current experimental research only one FRP RC girder was tested. Therefore, the authors found that it may not be reasonable to compare the values of ductility indices of BFRP RCB girder (calculated using the Energy-based approach or the Deformation-based approach) with those of steel and hybrid RCB girders (calculated by the traditional approach). Accordingly, the ductility index of the FRP RCB girder was not considered in this study and the conclusions were drawn depending on the strength and energy absorption of the girders in addition to their cracking and failure states.

Analyzing the test results of the current study showed that the hybrid RCB girders (BSF-0.33F, BSF-0.50F, as well as BSF-0.67F), having similar overall area of reinforcement, failed because of steel yielding followed by the rupture of BFRP bars. Also, test results showed that the hybrid RCB girders absorbed much more energy than that of the BF girder. This long-established the advantage of substituting parts of BFRP bars with steel bars in the tension region as they increase the absorbed energy and hence advance the ductility of these box girders, as it is specified in Table 6 as well as revealed in Figs. 7 and 10. It could be also indicated that as the A_f/A_t ratio lessened, the ductility index increased; i.e., the A_f/A_t ratio is an important factor controlling the deformability of hybrid RCB girders.

By combining the analysis of ductility index with the strength and failure modes of the test specimens, it is observed that for all box girders reinforced with BFRP or mixed bars (BFRP and

steel bars), the BFRP bars ruptured at failure because the strain in these bars came to its ultimate value, which means that the examined RCB girders had under-reinforced sections. To evade this kind of brittle failure, hybrid RCB girders ought to have over-reinforced sections with greater strength, stiffness, as well as ample ductility. Established on the existing test outcomes, the ratio A_f/A_t must be inside the assortment of 50% to 70% to deliver an adequate amount of post elastic strength as well as stiffness for meeting the ductility requirements.

As for the energy absorption and referring to the work done by Arivalagan and Kandasamy [42], the energy absorption (EA) capacities are assessed by computing the area below the load-midspan deflection curves as presented in Fig. 11. The values of the EA capacities of the examined girders are presented in Table 6. The BF box girder acquired the least EA capacity of 9.4 kN.m, while the maximum EA capacity of 16.7 kN.m was documented for the BS sample as displayed in Fig. 12 as well as Table 6. Comparing with the reference girder, the EA values reduced by 13.3% to 43.6%, where the reduction value increased with increasing the FRP reinforcement ratio.

Table 6: Energy absorption and ductility index of the tested specimens.

Girder ID	A_f/A_t ratio	EA (kN.m)	Decrease in EA (%)	Δ_y (mm)	Δ_u (mm)	μ_D (Δ_u/Δ_y)
BS	0.00	16.7	-	7.4	80	10.8
BSF-0.33F	0.33	14.4	13.3	7.6	62	8.2
BSF-0.50F	0.50	14.1	15.3	8.0	57	7.1
BSF-0.67F	0.67	12.7	23.7	8.2	54	6.6
BF	1.00	9.4	43.6	-	52	-

EA is the energy absorption; Δy and Δu stand for yielding and ultimate deflection, respectively; and μD = Ductility index.

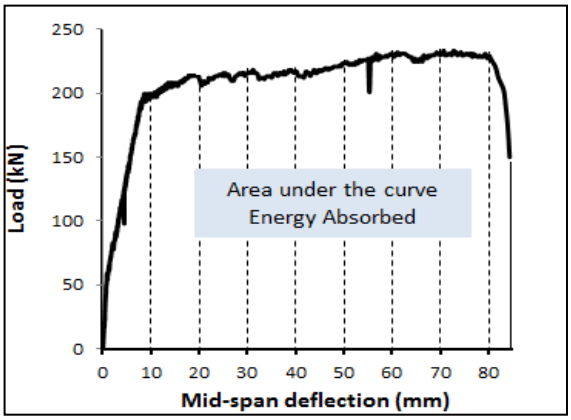

Fig. 11. Typical load-displacement curves for evaluating the energy absorption (EA).

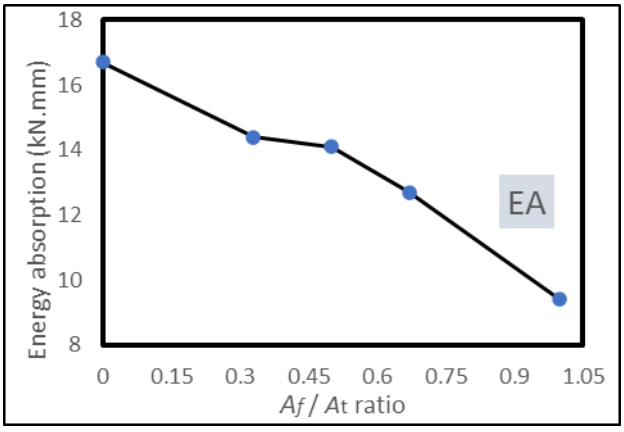

Fig. 12. Energy absorption (EA) capacity of the tested specimens.

4.3. Effect of A_f/A_t ratio on the induced strains of both steel and BFRP reinforcements

The tensile strain in the main longitudinal reinforcement was measured at midspan for the tested girders. Through Figs. 13, 14, and Table 4, it is obvious that for the reference girder BF, the increase in strain after the first crack up to about 50% of the ultimate load is more than that in girder BS, which is reinforced with steel bars only. Also, from these figures, the measured strain at failure of the hybrid girders is slightly larger than that in girder BS. The strain in steel bars at failure for all girders reached its yield value, and the strain in BFRP bars reached its ultimate value.

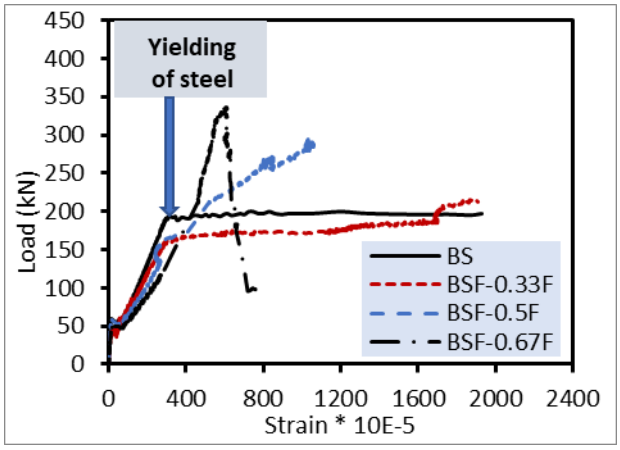

Fig. 13. Load-main steel reinforcement strain curves.

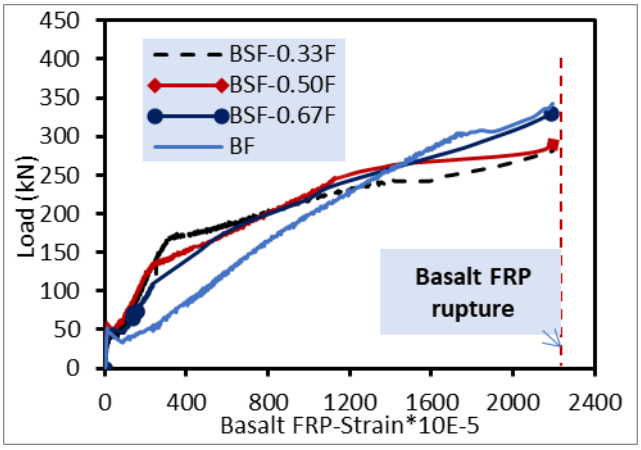

Fig. 14. Load-main BFRP reinforcement strain curves.

5. Analytical Evaluation of the Flexural Capacity of the Tested Girders

Precise analytical predictions of the flexural capacity of structural elements play a significant role in the evaluation and design of such elements. Therefore, this section addresses the application of the structural equations as well as models available in the literature to evaluate analytically the flexural capacity of hybrid RCB girders.

5.1. Modes of failure

Examination outcomes from the literature exhibited that the steel bar primarily offers stiffness as well as ductility, whereas the FRP bar offers great strength as well as durability for the hybrid-RC cross sections. Nonetheless, too much FRP bar application may cause crushing failure of the concrete prior to the steel yielding, however insufficient FRP bars could result in brittle failure due to rupture of the FRP bars. Henceforth, the failure mode of the components is considerably affected by the effective reinforcement ratio as well as the A_f /A_t ratio for hybrid RCB girders. For hybrid-RC beams, numerous failure modes control the structural performance of such members. Rendering to (Pang et al. 2016) [29], Table 8 summarized the failure modes of flexural hybrid-RCB girders. The effective reinforcement stiffness $\rho_{sf.s}$ as well as the mechanical reinforcing index $\rho_{sf.f}$ presented in Table 8 are demarcated as follows:

$$\rho_{sf.s} = \frac{E_s A_s + E_f A_f}{E_s bd} = \rho_s + \frac{E_f}{E_s}\rho_f \quad (1)$$

$$\rho_{sf.f} = \frac{f_y A_s + f_{fu} A_f}{f_{fu} bd} = \rho_s \frac{f_y}{f_{fu}} + \rho_f \quad (2)$$

When concrete crushing as well as steel yielding take place simultaneously though the FRP bars have not ruptured so far, the yield reinforcement ratio $\rho_{s.b}$ can be calculated by the ACI 440.1 R-03 [20] equation:

$$\rho_{s.b} = 0.85\beta_1 \frac{f'_c}{f_y} \frac{E_s \varepsilon_{cu}}{f_y + E_s \varepsilon_{cu}} \quad (3)$$

The critical reinforcement ratio $\rho_{f.b}$ can be calculated as the reinforcement ratio when concrete crushing and FRP bar rupturing occur simultaneously after the steel rebars have yielded by the ACI 440.1 R-03 [20] equation:

$$\rho_{f.b} = 0.85\beta_1 \frac{f_c'}{f_{fu}} \frac{E_f \varepsilon_{cu}}{E_f \varepsilon_{cu} + f_{fu}} \quad (4)$$

whereas $\beta 1$ = ratio of the depth of equivalent rectangular stress block to the depth of the neutral axis; E_s = elastic modulus of the steel reinforcement; A_s = cross sectional area of the steel bars; E_f = elastic modulus of the FRP; A_f = cross sectional area of the FRP bars; b = breadth of the beam and d = distance from the extreme compression fiber to the centroid of the tension reinforcing region; $\rho_s = \frac{A_s}{bd}$ = steel reinforcement ratio; $\rho_f = \frac{A_f}{bd}$ = FRP reinforcement ratio; f_y = specific yielding stress of the steel reinforcement; f_{fu} = ultimate tensile strength of the FRP reinforcement; f_c' = cylinder compressive strength of the concrete; in addition to ε_{cu} = 0.003 = extreme fiber concrete compressive strain.

Table 8: Failure Modes of the Flexural Hybrid-RCB girders [24].

Failure mode	Control material	Demanded reinforcement condition	Remarks
Concrete crushing, steel nonyielding, FRP non-rupturing	Concrete	$\rho_{sf.s} > \rho_{s.b}$	Inadmissible
Steel yielding, concrete crushing, FRP rupturing	Steel and concrete	$\rho_{sf.s} \leq \rho_{s.b}$ and $\rho_{sf.f} \geq \rho_{f.b}$	Permissible
Steel yielding, FRP rupturing, concrete non-crushing	FRP and steel bars	$\rho_{sf.f} < \rho_{f.b}$	Inadmissible

Because of the small elastic modulus and great ultimate strength of FRP bars, the critical reinforcement ratio is much lesser than the yield reinforcement ratio, $\rho_{f.b} < \rho_{s.b}$.

When the $\rho_{sf.f} \geq \rho_{f.b}$, as well as the $\rho_{sf.s} \leq \rho_{s.b}$, flexural failure of the box girder initiates with steel yielding, heralded by concrete crushing, then finally FRP bar rupturing ($\varepsilon_c = \varepsilon_{cu}$, $\varepsilon_y < \varepsilon_s = \varepsilon_f \leq \varepsilon_{fd}$) as specified in Table 8. The section is under-reinforced, which is a favored methodology in the design of hybrid-RCB girders for its elastic failure.

The FRP bars have no strength held in reserve if the $\rho_{sf.f} < \rho_{f.b}$, as the components are constructed to fail once FRP ruptures. Concrete plastic deformation is not observable in this kind of members ($\varepsilon_c < \varepsilon_{cu}$, $\varepsilon_{fd} < \varepsilon_s = \varepsilon_f$). Consequently, this circumstance is not permitted in a practical construction for its brittle failure.

As soon as the $\rho_{sf.s} > \rho_{s.b}$, the longitudinal bar strain is small ($\varepsilon_c = \varepsilon_{cu}$, $\varepsilon_s = \varepsilon_f < \varepsilon_y = f_y / E_s$), and the concrete strain in the compression region has come to the ultimate level. Concrete crushing will control the failure mode. This condition is similar to over-reinforced concrete beams and is also not endorsed in practical construction for its brittle failure.

5.2. Prediction of Ultimate Flexural Capacity

The flexural capacity of the girders in the current study was calculated based on the hypothesis of a plane cross-section before bending remain plane after bending. Moreover, as well as a composite

action of both concrete and reinforcing bars is developed with a perfect bond between the two components. The stress in tensile FRP bar was quantified by means of force equilibrium, strain compatibility, as well as the ACI 440.1 R-03 [19], existing provisions available in the literature [32-33]. Rectangular stress block suggestion for the stress distribution in compressive concrete, the stress in tensile FRP bars (f_f) as well as the nominal moment capacity (Mu) in the ultimate limit state can be premeditated referring to Qu et al. 2009 [32] by employing Eqs. (5) and (6).

$$f_f = \sqrt{\frac{1}{4}\left(\frac{A_s f_y}{A_f} + E_f \varepsilon_{cu}\right)^2 + \left(\frac{0.85 B_1 f_c'}{\rho_f} - \frac{A_s f_y}{A_f}\right) E_f \varepsilon_{cu}} - 0.5\left(\frac{A_s f_y}{A_f} + E_f \varepsilon_{Cu}\right) \quad \subseteq f_{fu} \tag{5}$$

$$M_u = \rho_f f_f + \rho_s f_y \left(1 - 0.59 \frac{\rho_f f_f + \rho_s f_y}{f_c'}\right) b d^2 \tag{6}$$

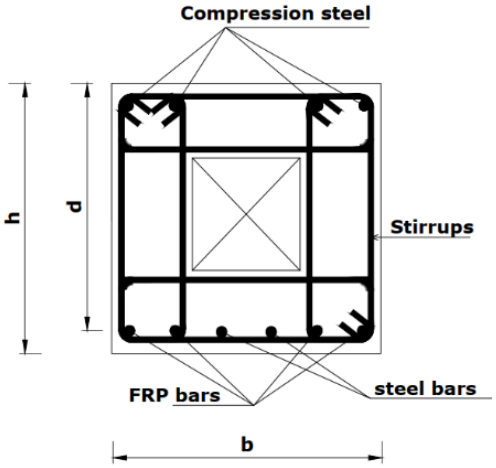

Fig. 15. Cross-sectional details of the proposed hybrid-RC box girders.

Table 9 compares the theoretical moment capacity with the experimentally calculated ones ($M_{u.exp}$) of the hybrid-RC box girders examined in this study. As shown in Table 9, the average ratio of the theoretical moment to the experimental ones for the 3 under-reinforced hybrid box girders is 0.987, demonstrating that the proposed model for the flexural strength of hybrid-RCB girders is conservative and can be applied in design procedures. Also, such agreement assures the strong composite action between BFRP bars and concrete.

Table 9: A comparison between the analytical and experimental flexural capacities of the tested girders.

Girder ID	$M_{u.exp}$ (KN. m)	$M_{u.th}$ (KN .m) Eq. (6)	$M_{u.th}$ / $M_{u.exp}$	$\rho_{sf.s}$% Eq. (1)	$\rho_{sf.f}$% Eq. (2)	$\rho_{s.b}$ % Eq. (3)	$\rho_{f.b}$ % Eq. (4)	Remarks
BS	139.8	122	0.880	0.45	-	2.27	-	Under-reinforced
BSF-0.33F	168	160	0.950	0.37	0.29	2.27	0.226	
BSF-0.50F	177.6	181.4	1.020	0.28	0.33	2.27	0.226	
BSF-0.67F	201	199.4	0.990	0.22	0.37	2.27	0.226	
BF	210	230	1.095	-	0.45	-	0.226	

Where $M_{u.exp}$ is the measured moment obtained from the experimental tests, $M_{u.th}$ is the theoretical moment capacity, $\rho_{sf.s}$ *is the effective* reinforcement stiffness whilst the mechanical reinforcing index $\rho_{sf.f}$. $\rho_{s.b}$ *is* the yield reinforcement ratio of steel bars, also $\rho_{f.b}$ *is the* critical reinforcement ratio of FRP bars.

6. Conclusions

The structural performance of hybrid (BFRP and steel) RCB girders has been investigated in this study. Through experimental investigations on 5 RCB girders, the influence of the key parameter (A_f/A_t ratio) on the flexural behavior of the girders was assessed. The characteristics of cracking and failure modes, cracking and ultimate strengths, deformability and ductility of the girders were evaluated. The ultimate flexural capacity of the girders was finally predicted through analytical calculations. Based on the test results as well as the analytical calculations, the following findings could be concluded:

1. Comparing with BFRP RCB girders, combining steel bars and BFRP bars improved both the strength and deformability of the girders.
2. For a constant total reinforcement ratio, the increase of A_f/A_t ratio amplified the crack height, ultimate load as well as deflection at failure, whereas the ductility index declined. For instance, the crack height of hybrid girders possessing an A_f/A_t ratio equivalent to 0.33, 0.50, and 0.67 was 71%, 83%, and 90% of that of the BFRP girder possessing an A_f/A_t ratio equivalent to zero, respectively.
3. All the examined hybrid girders failed because of the rupture of BFRP following yielding of steel bars, as well as crushing of concrete; whereas the reference girder that were strengthened with solely steel bars, failed by concrete crushing in the compressive region following yielding of steel bars.
4. Hybrid RCB girders ought to encompass a great percentage of FRP bars to evade quick rupture of those bars. An A_f/A_t ratio inside the range of 50% to 70% is commended in the design of similar girders to deliver sufficient post elastic strength as well as stiffness for meeting the ductility demand.
5. Analytical estimations of the ultimate flexural capacity of the examined girders compared well with the examination outcomes, which indicates the adequate BFRP-concrete composite action.

Due to the high cost of laboratory tests on the concrete box girders, especially those reinforced with hybrid steel and FRP reinforcements and because of the limited materials available in the Egyptian market, the authors could only prepare and test 5 represented specimens. The study is, therefore, to be continued through a wide numerical parametric study to precisely understand the fundamental characteristics of the proposed system, optimize the A_f/A_t ratio, and investigate the influence of other parameters.

References

[1] Luís João Ferreira Vieira, Longitudinal Analysis of Steel-Concrete Composite Box Girder Decks: Comparison between the Classical Formulations and the Generalized Beam Theory, M. Sc Thesis,

[2] Yuliang He, KaiWang, Zongyong Cao, Peijuan Zheng, and Yiqiang Xiang, Reinforcement Analysis of an Old Multi-Beam Box Girder Based on a New Embedded Steel Plate (ESP) Strengthening Method, J. Materials 2022, 15, 4353. https://doi.org/10.3390/ma15124353

[3] Yousry B.I. Shaheen, Boshra Eltaly, and Amany Henish, Response of Reinforced Concrete Box Girders Strengthened with composite Materials, J. Research Square (2022), DOI: https://doi.org/10.21203/rs.3.rs-1666445/v1

[4] Savio John and Reshma Prasad, AN OVERVIEW ON BOX GIRDER BRIDGES, International Research Journal of Engineering and Technology (IRJET) 4(2017) 522-524.

[5] Mayank Chourasia and Saleem Akhtar, Design and Analysis of Prestressed Concrete Box Girder by Finite Element Method (4 Cells & 1 Cell), International Journal of Civil and Structural Engineering Research, 3 (2015) 413-421.

[6] Askar R. A. and Abd–Alkhalek M., (2012) "Response of R.C. Box Girders Strengthened using CFRP Sheets," Journal of American Science, Vol. 8, No.12.

[7] Mohamed Elsedemy, Mohamed Kandil, Nageh N. Meleka, A State-of-the-Art Review on the Behavior of RC Beams with Different Types of FRP Reinforcement, Engineering Research Journal, 45 (2022) 591-600.

[8] Ibrahim AMA, Wu Z, Fahmy MFM, Kamal D. Experimental Study on Cyclic Response of Concrete Bridge Columns Reinforced by Steel and Basalt FRP Reinforcements. J Compos Constr 2016; 20:04015062.

[9] Wu, Z. S., Fahmy, M. F. M., and Wu, G. (2009). "Safety enhancement of urban structures with structural recoverability and controllability." J. Earthquake Tsunami, 3(3), 143–174.

[10] Priestley, M., Seible, F., and Calvi, G. M. (1996). Seismic design and retrofit of bridges, Wiley, New York.

[11] Ashour AF. Flexural and shear capacities of concrete beams reinforced with GFPR bars. Constr Build Mater 2006; 20:1005–15.

[12] Ashour AF, Habeeb MN. Continuous concrete beams reinforced with CFRP bars. Struct Build 2008; SB6:349–57.

[13] Z. H. Awadallah, M. Ahmed, O. Farghal et al., "Some Parameters Affecting Shear Behavior of High Strength Fiber Reinforced Concrete Beams Longitudinally Reinforced with BFRP Rebars," JES. Journal of Engineering Sciences, vol. 42, no. 5, pp. 1163-1178, 2014.

[14] Barris C, Torres LI, Turon A, Baena M, Catalan A. An experimental study of the flexural behaviour of GFRP RC beams and comparison with prediction models. Compos Struct 2009; 91:286–95.

[15] Benmokrane B, Chaallal O, Masmoudi R. Glass fibre reinforced plastic (GFRP) rebars for concrete structures. Constr Build Mater 1995;9(6):353–64.

[16] Brown VL, Bartholomew CL. FRP reinforcing bars in reinforced concrete members. ACI Mater J 1993;90(1):34–9.

[17] F. Elgabbas, P. Vincent, E. A. Ahmed, and B. Benmokrane, "Experimental Testing of Basalt-Fiber-Reinforced Polymer Bars in Concrete Beams," Compos. Part B Eng., Vol. 91, pp. 205–218, Apr. 2016.

[18] M. El-Mogy, A. El-Ragaby, E. El-Salakawy, "Flexural behavior of continuous FRP-reinforced concrete beams" J. Compos. Constr. 14 (6) (2010) 669–680.

[19] S. Sirimontree, S. Keawsawasvong, and C. Thongchom, "Flexural Behavior of Concrete Beam Reinforced with GFRP Bars Compared to Concrete Beam Reinforced with Conventional Steel Reinforcements," J. Appl. Sci. Eng., Vol. 24, No. 6, pp. 883–890, 2021.

[20] ACI 440.1R-15. Guide for the design and construction of structural concrete reinforced with fiber-reinforced polymer (FRP) bars. Farmington Hills, MI: ACI (American Concrete Institute), (2015). 83.

[21] CSA S806-12. Design and construction of building components with fibre-reinforced polymers. Rexdale, ON, Canada: CSA (Canadian Standard Association). (2012).

[22] M.A. Aiello, L. Ombres, Structural performances of concrete beams with hybrid (fiber-reinforced polymer–steel) reinforcements, J. Compos. Constr. 6 (2) (2002) 133–140.

[23] Ahmed El Refai, Farid Abed, Abdullah Al-Rahmani, Structural performance and serviceability of concrete beams reinforced with hybrid (GFRP and steel) bars, J. Construction and Building Materials 96 (2015) 518–529.

[24] Ibrahim HA, Fahmy MF. Finite-Element Analysis of Flexural Behavior of Hybrid Steel-FRP Continuous Reinforced Concrete (HSFCRC) Beams. The 6th Asia-Pacific Conference on FRP in Structures (APFIS2017). Singapore: The International Institute for FRP in Construction (IIFC); 2017.

[25] Ibrahim AMA, Fahmy MFM, Wu Z. 3D finite element modeling of bond-controlled behavior of steel and basalt FRP-reinforced concrete square bridge columns under lateral loading. Compos Struct 2016; 143:33–52.

[26] Haitham A. Ibrahim, Mohamed F.M. Fahmy, and Zhishen Wu, Numerical study of steel-to-FRP reinforcement ratio as a design-tool controlling the lateral response of SFRC beam-column joints, J. Engineering Structures 172 (2018) 253–274.

[27] I. F. Kara, A. F. Ashour, and M. A. Köroğlu, "Flexural Behavior of Hybrid FRP/Steel Reinforced Concrete Beams," Compos. Struct., Vol. 129, pp. 111–121, Oct. 2015.

[28] Lau D, Pam HJ. Experimental study of hybrid FRP reinforced concrete beams. Eng Struct 2010; 32:3857–65.

[29] Suzan A.A. Mustafa and Hilal A. Hassan, "Behavior of concrete beams reinforced with hybrid steel and FRP composites" HBRC Journal 14 (2018) 300–308.

[30] L. Pang, W. Qu, P. Zhu et al., "Design propositions for hybrid FRP-steel reinforced concrete beams," Journal of Composites for Construction, vol. 20, no. 4, pp. 04015086, 2016.

[31] Renyuan Qin, Ao Zhou, and Denvid Lau, "Effect of reinforcement ratio on the flexural performance of hybrid FRP reinforced concrete beams", J. Composites Part B, 108 (2017) 200-209.

[32] W. Qu, X. Zhang, H. Huang, Flexural behavior of concrete beams reinforced with hybrid (GFRP and steel) bars, J. Compos. Constr., ASCE 13 (5) (2009) 350–359.

[33] Xiangjie Ruan, Chunhua Lu, Ke Xu, Guangyu Xuan, Mingzhi Ni "Flexural behavior and serviceability of concrete beams hybrid reinforced with GFRP bars and steel bars," J. Composite structures, vol. 235, pp. 111772, 2020.

[34] M.A. Safan, Flexural behavior, and design of steel–GFRP reinforced concrete beams, ACI Mater. J. 110 (6) (2013) 677–685.

[35] AASHTO LRFD Bridge Design Specifications: US Customary Units: American Association of State Highway and Transportation Officials, 2010.

[36] Xue X, Wu M, Li Z and Zhou P 2020 Numerical analysis of dead load shear force distribution in webs of multicell inclined web box-girder bridge Advances in Civil Engineering 2020 pp 1-10

[37] Tvrtko Renić, and Tomislav Kišiček; "Ductility of Concrete Beams Reinforced with FRP Rebars" MDPI stays neutral regarding jurisdictional claims in published maps and institutional affiliations, 2021, 11, 424. https:// doi.org/10.3390/buildings11090424.

[38] R. Park, "Ductility evaluation from laboratory and analytical testing." pp. 605-616.

[39] Naani, A., "Flexural Behavior and Design of RC Members Using FRP Reinforcement," Journal of Structural Engineering, V. 119, No. 11, Nov. 1993, pp. 3344-3359.

[40] Jaeger GL, Tadros G, Mufti AA. "The concept of the overall performance factor in rectangular section reinforced concrete beams" Proc of 3rd int symp on non-metallic (FRP) reinforcement for concrete structures, vol. 2, Sapporo, Japan; 1997. p. 551–8.

[41] Victor C. Li and Shuxin Wang "Flexural Behaviors of Glass Fiber-Reinforced Polymer (GFRP) Reinforced Engineered Cementitious Composite Beams" ACI MATERIALS JOURNAL, 99 (2002) 11-21.

[42] K. Arivalagan, and K. Kandasamy, "Energy absorption capacity of composite beams," J. Eng. Sci. Technol. Rev, vol. 2, no. 1, pp. 145-150, 2009.

سلوك الانحناء للكمرات الخرسانية الصندوقية ذات التسليح المهجن

يعرض هذا البحث سلوك الانحناء للكمرات الخرسانية الصندوقية المسلحة بالحديد والبوليمرات المقواة بالألياف. تم إجراء دراسة عملية على خمسة كمرات صندوقية مسلحة. تم تسليح أول كمرتين في الناحية المعرضة للشد إما بأسياخ من حديد التسليح أو بأسياخ من البوليمرات المقواة بألياف البازلت، بينما تم تقوية الكمرات الثلاثة الأخرى بهجين من النوعين السابقين بنسب متنوعة. تم اختبار الكمرات تحت تحميل استاتيكي رباعي النقاط، وتم دراسة الخصائص الأساسية الرئيسية للتسليح المقترح. أظهرت النتائج العملية أن زيادة نسبة مساحة التسليح بأسياخ البوليمرات المقواة بألياف البازلت إلى مساحة التسليح الكلية تحسن كلا من الحمل الأقصى والترخيم عند الانهيار، بينما انخفض مؤشر الممطلوية. كشفت مقارنة نتائج اختبار الكمرات الخرسانية الصندوقية المسلحة التي تم الحصول عليها مع تلك الموجودة في المراجع للكمرات العادية أن السلوك تقريبًا متطابق. في نطاق المتغيرات العملية التي تم بحثها في هذه الدراسة، يوصى باستخدام قيمة تتراوح من حوالي ٥٠٪ إلى ٧٠٪ لنسبة مساحة التسليح بأسياخ البوليمرات المقواة بألياف البازلت إلى مساحة التسليح الكلية في تصميم الكمرات الخرسانية الصندوقية المسلحة الهجينة لأن هذه النسبة توفر من المقاومة والجساءة في مرحلة ما بعد المرونة ما يلبي متطلبات الممطولية. وفي النهاية تم تطبيق المعادلات الحسابية المتاحة في المراجع للتنبؤ بمقاومة الانحناء للكمرات الخرسانية الصندوقية المسلحة بالحديد والبوليمرات المقواة بالألياف وتم إثبات التوافق الجيد مع النتائج العملية.